



Baffle System Employing Reflective Surfaces

William I. Linlor

(NASA-TM-84406) BAFFLE SYSTEM EMPLOYING
REFLECTIVE SURFACES (NASA) 34 P
HC A03/MF A01

CSSL 20F

N84-13985

G3/74 Unclas
42731

December 1983

NASA Technical Memorandum 84406

Baffle System Employing Reflective Surfaces

William I. Linlor, Ames Research Center, Moffett Field, California

NASA

National Aeronautics and
Space Administration

Ames Research Center
Moffett Field, California 94035

SUMMARY

Reflective baffles are proposed to reject off-axis light entering a telescope. Toroidal surfaces and adjacent cones are positioned so that off-axis rays make multiple reflections between these two surfaces. Meridional rays are reflected approximately parallel to the entering direction. Skew rays are reflected obliquely, but leave the telescope aperture. The range of incident angles for which these reflections are obtained is approximately 45° . A system is described that is designed specifically for the Space Shuttle Infrared Telescope Facility (SIRTF). Because of its reflective properties, the proposed baffle system rejects about 90° of the heat load from the SIRTF sunshade that would be absorbed in systems of conventional black baffles.

INTRODUCTION

Telescopes serve to concentrate light on detectors such as photometers, spectrometers, bolometers, etc. Incoming light from sources out of the field of view can degrade the quality of the desired image, if such off-axis light is not suitably intercepted.

Baffles for telescopes operating in the visible-light wavelength region are coated with "optical blacks." Off-axis rays striking these surfaces are essentially absorbed; only a very small fraction is scattered. For such telescopes, the state of the art is highly developed, and the literature is extensive.

For telescopes in Earth orbit intended to operate in the infrared region, for example in wavelengths ranging from 1 to 1,000 μm (i.e., 10^{-6} to 10^{-3} m), "optical blacks" may fail to absorb incident radiation adequately. Additionally, such coatings can become detached from the baffles, thus contaminating the telescope, and the delicate nature of the surfaces may make refurbishment difficult.

This paper describes a baffle system that rejects off-axis radiation by reflecting it back out of the telescope. Another purpose of the system is to reduce the heat-loading of the telescope system. An intended application is in the Shuttle Infrared Telescope Facility (SIRTF), planned to be a helium-cooled telescope that will measure extremely faint radiation extending to the far-infrared wavelengths. A version of the telescope may be launched from the Shuttle and operated in the "free-flyer" mode; it would have a mission duration of 6 months or longer.

The thermal radiation from the SIRTF sunshade, if absorbed by the baffles, would constitute a major heat load and large, massive helium tanks would be needed to provide adequate cooling throughout the mission. The proposed baffle system is expected to absorb less than 10% of the thermal radiation from the sunshade. Solar radiation, if scattered into the telescope by the sunshade, is also reflected. The absorbed fraction, which depends on the angle of the Sun relative to the telescope axis, can be controlled by mission-dictated trajectories.

Recent papers (refs. 1 and 2) describe reflective baffle systems that are based on the properties of an ellipse. In the meridional plane, any ray entering between the two foci of an ellipse, then specularly reflected at the elliptical surface, must return between the two foci. Each elliptical baffle must have a different shape than the preceding one. For skew rays, about 10% of the incident radiation is not reflected back out of the telescope.

The reflective baffle system described in this paper is based on entirely different principles, and does not depend on the properties of an ellipse. Although many different types of surfaces can be employed, the present version uses toroidal surfaces together with adjacent cones to reflect radiation from the SIRTf sunshade (thermal emission or scattered sunlight).

The dimensions of the telescope and sunshade given in this paper, although nominally applicable to SIRTf, do not represent final design values.

REFLECTIVE BAFFLE SYSTEM

The elements of the present baffle system are shown in figure 1. The circular segment has a radius a , the center of curvature being at the origin of coordinates, located at the telescope wall. A line with the coordinates c, d makes an angle of A degrees with the x-axis. The telescope axis is at the right of the figure.

A baffle is produced by rotating this figure about the telescope axis. Upon such a rotation, the circular segment generates the surface of a torus, and the straight line generates the surface of a cone.

The explanation of the properties of this baffle system is facilitated by use of meridional rays, rather than skew rays. In the following material the meridional plane is implied, unless specifically stated otherwise. Sets of parameters that approximate the SIRTf telescope dimensions are employed.

Figures 2 through 10 illustrate the retro-reflective property of this baffle system for various conditions. In each case, the radius of the circular segment is 19.40 cm. The angle θ is the angle between the ray and the y-axis. The values of the parameters in figures 2-10 are listed in table 1.

Figure 2 shows that the reflected ray makes an angle of 25.78° with the telescope axis, the incident angle being 25.32° ; the increase in angle is approximately 0.5° . This is acceptable because, as shown below, the reflected rays either clear the telescope entirely, or impinge on a reflecting surface from which they leave the telescope.

Figures 3 through 7 show the effect of increasing angle A . In each case the reflected ray is nearly parallel to the incident ray, the difference in angle being less than 0.3° . In figure 5, only one ray is shown, because the reflected ray is essentially superimposed on the incident ray (the calculated angular deviation is only 0.01°).

In figures 8-10, angle A is constant at 44.53° . The angle of the incident ray is successively 50.00° , 60.00° , and 87.67° ; the reflected ray in each case is within 0.3° of parallelism with the corresponding incident ray. The break in the straight

line shown at $x = 5$ cm is necessary to prevent the intersection of the straight and curved lines.

As table 1 and figures 2-8 show, the parameters A and d differ for each figure. The question naturally arises as to the principle of operation of the system, and the basis for selection of parameter values. Because of its length and complexity, a rigorous treatment of the analysis is planned for a subsequent publication. For the present only a qualitative explanation is appropriate.

For the configuration shown in figure 1, the reflection properties depend on the parameters A and d , and on the shape of the curved segment; the latter is the circular segment in figure 1. To achieve less deviation in angle between the incident and reflected rays, the curved segment, instead of being circular, can be parabolic, elliptic, or a more complicated curve. The straight line in figure 1 can similarly be replaced by a more suitable curve. The present configuration is the simplest case of retro-reflectors based on multiple reflection between adjacent surfaces.

One can mathematically describe the multiply reflected ray path from the point of incidence to the point of emergence, and obtain expressions for the difference in the angles of the incident and emergent rays, in terms of the relevant parameters. Using differential calculus to minimize the angle-difference for an individual baffle set, one obtains the corresponding values of parameters, such as A , a , and d . Because the parameter d is a function of position along the telescope axis, similar treatment is necessary to optimize the performance of an array of baffle sets of the telescope.

In lieu of such a rigorous analysis, ray paths are calculated for a proposed SIRTf configuration to show that all radiation from the sunshade in the meridional plane is reflected back out of the telescope.

The behavior of skew rays requires the solution of a fourth-degree algebraic equation to determine each intersection point of a ray and the torus surface, which places a limitation on the number of skew rays that can be conveniently analyzed. A thorough skew-ray analysis is planned employing a computer and a suitable code.

REFLECTIVE BAFFLES FOR SIRTf

The existing SIRTf design is described in two reports (refs. 3 and 4) based on the "Phase A Concept Description," which is a summary of the science rationale and SIRTf concepts (ref. 5).

The existing SIRTf telescope is shown in the simplified sketch in figure 11, which defines the telescope-based coordinate system. Capital letters X and Y are used to distinguish this system from the previously defined baffle coordinate system. The location $Y = 0$ is the point at which the ray incident at an angle of 23.00° with the Y -axis intersects the telescope barrel. The location $X = 0$ is the telescope axis. The telescope barrel has the nominal radius of 52.00 cm and extends along the Y -axis to 233.60 cm. The sunshade is identified by the lines EF and FG , whose coordinates are shown in the sketch.

For purposes of this paper the SIRTf sunshade is modified as shown in figure 12. The angle of the baffle GH (assumed to be at the helium-cooled temperature of the telescope) is equal to that of the limiting ray that can enter the telescope, namely

24.386° with the Y-axis, based on the dimensions given in figure 12, which are selected to provide the baffle GH with an extent along the Y-axis of 30.00 cm. When this design was initiated, the dimensions for baffle GH, necessary to reflect all meridional rays, were not known. For the present design of baffle GH, the Sun must have an off-axis angle of 52.00° or more to prevent its rays from striking the baffle GH. If the Sun is at an angle of 45°, the rays are reflected as shown in figure 13, without entering the telescope.

The values given in figures 11-13 are illustrative only, and are intended to be internally consistent so that (based on geometrical optics) all radiation emitted by the sunshade that is incident on the baffles is reflected back out of the telescope. The dimensions of the telescope and the values of the parameters are preliminary. Further analysis and trade-off factors must be considered to determine the best values. The use of four integers following the decimal point is intended solely to avoid round-off errors, and to help identify lines and angles.

In the telescope application, each baffle consists of a straight and a curved line that are tangent to each other at the point of contact, as illustrated in figure 14. The two coordinate systems (associated with the baffles and with the telescope) are combined in this figure. The location of the center of curvature for each circular segment is given in the Y-coordinate system by the parameter R.

To distinguish between two adjacent baffles the convention is adopted that parameters for the upper set have the subscript "a" and parameters for the lower set have the subscript "b." Thus, for figure 14 the parameter sets are:

$Y_a = 213.9136 \text{ cm}$	$Y_b = 207.8960 \text{ cm}$
$R_a = 199.8149 \text{ cm}$	$R_b = 193.5601 \text{ cm}$
$A_a = 43.3863^\circ$	$A_b = 42.3568^\circ$
$c_a = 13.3261 \text{ cm}$	$c_b = 13.0707 \text{ cm}$
$d_a = 7.7581 \text{ cm}$	$d_b = 8.0811 \text{ cm}$

The origin of coordinates for figure 14 is $y = 0$; this is also the same as $Y = 199.8149$. In the y -system, the parameter $d_b = 8.0811$, which corresponds to $Y = 207.8960$.

The relation between R, Y, and A is as follows:

$$R_a = Y_a - 19.400 \cos A_a$$

$$Y_b = R_a + d_b$$

Seven sets of baffles are shown in figure 15. The baffle GH of figure 12 is shown at the top of figure 15, making the angle of 65.6140° with the X-axis. All of the remaining baffles have angles less than 45° with the X-axis. The coordinate system used in figure 15 is a hybrid one; that is, values for the ordinates are given in the Y-coordinates; values for x are relative to the wall where $x = 0$.

The parameters for the 37 sets of baffles for the SIRTIF telescope are given in table 2.

MERIDIONAL RAY REFLECTION

The following description is based on meridional ray paths. The present calculation is concerned with the displacement along the Y-axis of a ray composed of two parts. The first is the ray displacement caused by its bounces between the two reflecting surfaces; this is defined to be "DELTA Y":

$$\text{DELTA Y} = y_{\text{out}} - y_{\text{in}}$$

A positive value for DELTA Y means that the ray has been displaced toward the telescope aperture.

The second contribution to the displacement along the Y-axis, defined to be "UP Y," is produced by the net angular deviation of the ray multiplied by the diameter of the telescope. This is true for all baffle locations along the Y-axis. With the net angular deviation of a ray expressed in degrees and a telescope diameter of 104.00 cm, the relations are

$$\text{DELTA } \theta = \theta_{\text{in}} - \theta_{\text{out}}$$

$$\text{UP Y} = 1.815 \text{ DELTA } \theta$$

The above definition for DELTA θ is chosen so that a positive sign signifies that the displacement is toward the telescope aperture (i.e., in the same direction as for a positive value for DELTA Y).

The net displacement of the ray is given by the sum of DELTA Y plus UP Y, and is defined to be "NET Y":

$$\text{NET Y} = \text{DELTA Y} + \text{UP Y}$$

The relationship of the net ray displacement to the baffle GH is now considered.

Any point on the sunshade is a source of off-axis radiation, such as point F in figure 12. It is of no consequence whether the reflected radiation is returned to a point above or below F, as long as it is above point G. Since point G represents the transition from the sunshade region (at a temperature of about 200 K) and the baffle region (at a temperature determined by the liquid-helium), in effect no radiation is emitted below point G. Thus, radiation from point G is the limiting point of off-axis radiation.

The baffle GH makes an angle of 24.386° with the telescope axis, and extends from $Y = 250.00$ cm to $Y = 220.00$ cm, yielding a distance of 30.00 cm along the Y-direction. This is the maximum negative value for NET Y that is permissible, consistent with the requirement that the returned ray must strike the baffle GH, from which it is then reflected out of the telescope.

Stated alternatively, the baffle GH provides a displacement distance of 30.00 cm as being the permissible maximum-negative value for NET Y for a ray. If any ray has a value of NET Y that exceeds 30.00 cm, it is not reflected back out of the telescope.

In order to determine the values of NET Y, meridional ray paths have been calculated for all 37 baffle sets, for all physically permissible incoming ray angles, and for points of incidence on the baffles. Examination of these results shows that the maximum downward (i.e., negative) value of NET Y is less than 5 cm. This is well within the available distance of 30 cm.

Because a tabulation of the calculated points involves many numbers that do not portray the trends, data are plotted in figures 16-20 to display the relations.

For three values of incoming-ray angles, the dependence of DELTA Y and DELTA θ on the value of x is shown in figures 16 and 17. Although the curves differ in detail, the conclusion is that the greatest excursions of the rays are essentially independent of the incoming-ray angle.

The effect of baffle location in the telescope is shown in figures 18-20, which show, respectively, DELTA Y, DELTA θ , and NET Y for the conditions listed in table 3.

The maximum excursion of NET Y (fig. 20) is seen to be less than 5 cm. Because this maximum downward (i.e., negative) value of NET Y is less by a factor of 6 than the distance of 30 cm available along baffle GH for reflecting rays out of the telescope, the conclusion is justified that all of the meridional rays are reflected back out of the telescope.

The preceding analysis represents the initial set of parameters. It is likely that some modification may result in a decrease in the magnitude of the NET Y values, and the sunshade dimensions may be modified to reduce the minimum off-axis Sun angle. Of course, sensitivity and manufacturing-tolerance considerations must be included in such analyses.

SKEW RAYS

The analysis of the paths of skew rays is much more complicated than that of meridional rays. To obtain the intersection point of a ray with the surface of the torus, solution of a fourth-degree equation is necessary. Details of the skew-ray analysis, with equations and results, must be deferred for a later paper.

Several hundred typical skew rays' paths have been analyzed for the SIRTIF configuration. All of these rays are reflected back out of the telescope. The conclusion is justified that the present baffle system can reflect incident radiation very well. Verification of this conclusion will be obtained by the use of a computer ray-tracing calculation that will examine the paths of rays incident on the baffle cavities in a dense grid pattern, for selected angles within the entrance region.

To state the conclusion more precisely, a three-dimensional coordinate system is useful.

Let the telescope axis be the Z-axis, with the X- and Y-axes lying on the plane perpendicular to the telescope axis. The angle of the incident ray with the Z-axis is the angle θ_{in} . After typically six reflections within the baffle cavity, the ray emerges at an angle θ_{out} . The difference between these two angles is sufficiently small so that the rays are reflected from the telescope. The situation can be represented by use of a cone having angle θ_{in} , on whose surface the incident ray

is located. The emergent ray is located on the surface of essentially the same cone, but with the vertex at a different location on the lower baffle surface.

If it is desired to limit the excursion of the cone vertex, the rays can be "compartmentalized." Polished spacers parallel to the Z-axis can be located every 30° in azimuth, so that a total of 12 such spacers are present for each set of curved baffles. These spacers serve to maintain the rigidity of the curved baffles as well as to "compartmentalize" the ray paths. Such spacers would be recessed a few centimeters away from the circular edge of the curved baffles to minimize scattering paths along the Z-axis.

HEAT LOAD ON BAFFLES

The heat load on the baffles produced by thermal radiation from the SIRTTF sunshade can be approximated by assuming that each ray makes a total of six reflections between the baffle surfaces, and then is returned back out of the telescope.

For the sunshade temperature of 200 K, the peak of the Planck radiation distribution occurs at about 15 μm . At this wavelength and at the temperature of 10 K (SIRTTF forebaffle cooled liquid helium) a gold-plated reflector has the theoretical absorptivity of 10^{-3} , based on data from the International Critical Tables. For the corresponding reflectivity of 0.999 and six reflections, the net reflectivity is equal to 0.99. Allowing for surface contamination and similar effects, which may reduce the reflectivity by unknown amounts, the conservative conclusion is that the net reflectivity may be reduced to 0.90, for which the heat load on the baffles is about 10% of the amount if all of the rays incident on the baffles are absorbed.

REFERENCES

1. Rock, D. F.; Warren, A. D.; and Lewanski, A. J.: Use of Reflective Baffles for Control of Aperture Heat Loads and Stray Radiation. Optical Systems Engineering, Proceedings of SPIE, vol. 330, Jan. 1982, pp. 60-65.
2. Bremer, J. C.: Baffle Design for Earth Radiation Rejection in the Cryogenic Limb-Scanning Interferometer/Radiometer," Optical Engineering, vol. 22, no. 1, Jan.-Feb. 1983, pp. 166-171.
3. SIRTF System Design Summary Document. Perkin-Elmer Corp., Contract NAS2-10066 for Ames Research Center, Aug. 1979.
4. SIRTF Design Optimization Study. Final technical report, Perkin-Elmer Corp., Contract NAS2-10066 for Ames Research Center, Sept. 1979.
5. SIRTF Infrared Telescope Facility, Phase A Concept Description. Ames Research Center, Aug. 28, 1981.

TABLE 1.- BAFFLE SYSTEM PARAMETERS^a

Figure	A, deg	c, cm	d, cm	θ_{in} , deg	θ_{out} , deg	$\theta_{in} - \theta_{out}$, deg
2	23.47	7.73	9.90	25.32	25.78	-0.46
3	29.50	9.70	11.25	43.00	43.01	-0.01
4	30.67	9.90	11.08	40.00	39.98	0.02
5	32.26	10.36	10.80	45.00	45.01	-0.01
6	33.77	10.78	10.00	50.89	50.84	0.05
7	38.81	12.16	8.90	67.88	68.15	-0.27
8	44.53	13.61	7.40	50.00	49.92	0.08
9	44.53	13.61	7.40	60.00	60.27	-0.27
10	44.53	13.61	7.40	87.67	87.80	-0.13

^aSee figure 1 and corresponding text for definitions of variables.

ORIGINAL PAGE IS
OF POOR QUALITY

TABLE 2.- SYSTEM PARAMETERS FOR SIRTFF BAFFLE SETS

Baffle set	Y	R	A	c	d
1	220.0000	206.1556	65.6140	13.5901	
2	213.9136	199.8149	43.3863	13.3261	7.7581
3	207.8960	193.5601	42.3568	13.0707	8.0811
4	201.9451	187.3878	41.3771	12.8236	8.3849
5	196.0581	181.2939	40.4439	12.5848	8.6703
6	190.2318	175.2739	39.5542	12.3541	8.9379
7	184.4623	169.3230	38.7049	12.1310	9.1884
8	178.7454	163.4357	37.8933	11.9153	9.4224
9	173.0762	157.6065	37.1165	11.7067	9.6405
10	167.4499	151.8293	36.3723	11.5048	9.8434
11	161.8609	146.0981	35.6580	11.3092	10.0315
12	156.3035	140.4065	34.9716	11.1195	10.2054
13	150.7720	134.7478	34.3110	10.9355	10.3655
14	145.2600	129.1153	33.6742	10.7567	10.5122
15	139.7612	123.5019	33.0593	10.5828	10.6459
16	134.2688	117.9006	32.4648	10.4136	10.7668
17	128.7758	112.3038	31.8890	10.2486	10.8752
18	123.2751	106.7040	31.3305	10.0875	10.9713
19	117.7591	101.0932	30.7878	9.9301	11.0551
20	112.2200	95.4632	30.2597	9.7760	11.1268
21	106.6496	89.8056	29.7448	9.6251	11.1863
22	101.0392	84.1115	29.2422	9.4769	11.2336
23	95.3798	78.3714	28.7506	9.3314	11.2684
24	89.6620	72.5758	28.2691	9.1881	11.2905
25	83.8755	66.7141	27.7967	9.0469	11.2997
26	78.0097	60.7756	27.3324	8.9076	11.2956
27	72.0531	54.7484	26.8754	8.7698	11.2775
28	65.9933	48.6203	26.4248	8.6334	11.2449
29	59.8173	42.3776	25.9797	8.4982	11.1970
30	53.5106	36.0062	25.5394	8.3640	11.1329
31	47.0578	29.4902	25.1031	8.2304	11.0516
32	40.4420	22.8127	24.6701	8.0974	10.9518
33	33.6447	15.9551	24.2395	7.9647	10.8320
34	26.6457	8.8969	23.8107	7.8321	10.6906
35	19.4224	1.6157	23.3829	7.6994	10.5255
36	11.9502	-5.9135	22.9553	7.5663	10.3345
37	4.2012	-13.7185	22.5273	7.4326	10.1148

ORIGINAL PAGE IS
OF POOR QUALITY

TABLE 3.- CURVES FOR DELTA Y,
DELTA θ , AND NET Y

Curve ^a	Y_a	Y_b	θ
A	220.0000	213.9136	70.00
B	207.7960	201.9451	65.00
C	196.0581	190.2318	60.00
D	184.4623	178.7454	55.00
E	173.0762	167.4499	51.00
F	134.2688	128.7758	40.00
G	83.8755	78.0097	31.00
H	59.8173	53.5106	27.00

^aLetters correspond to curves
shown in figures 18, 19, and 20.

ORIGINAL PAGE IS
OF POOR QUALITY

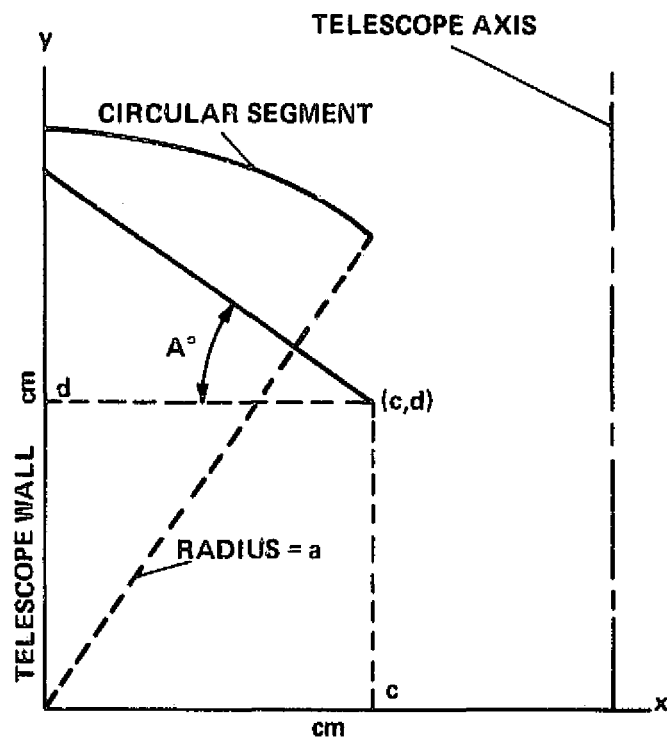


Figure 1.- Reflective baffle geometry.

ORIGINAL PAGE IS
OF POOR QUALITY

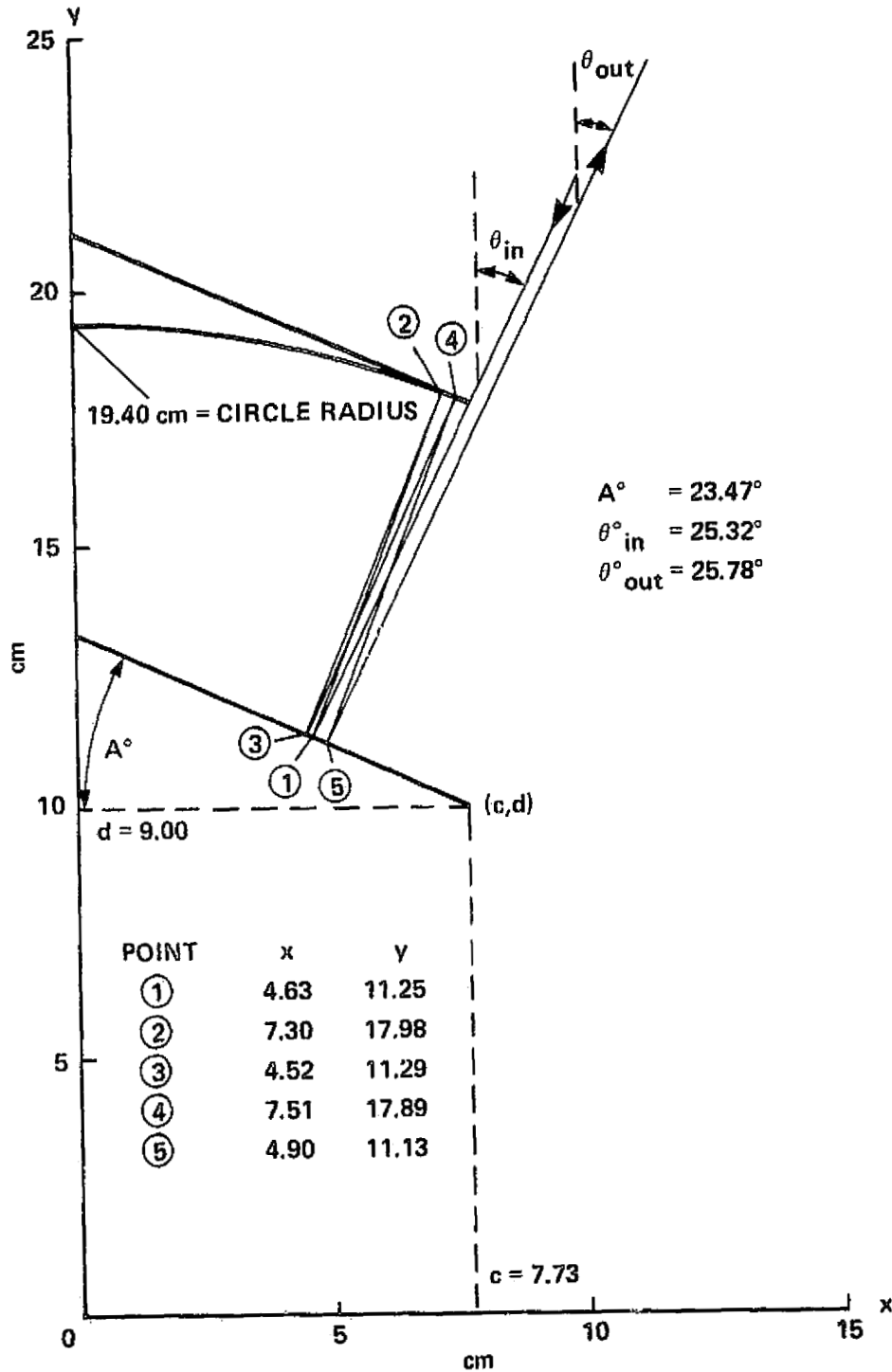


Figure 2.- Ray reflections for baffle angle of 23.47° .

ORIGINAL PAGE IS
OF POOR QUALITY

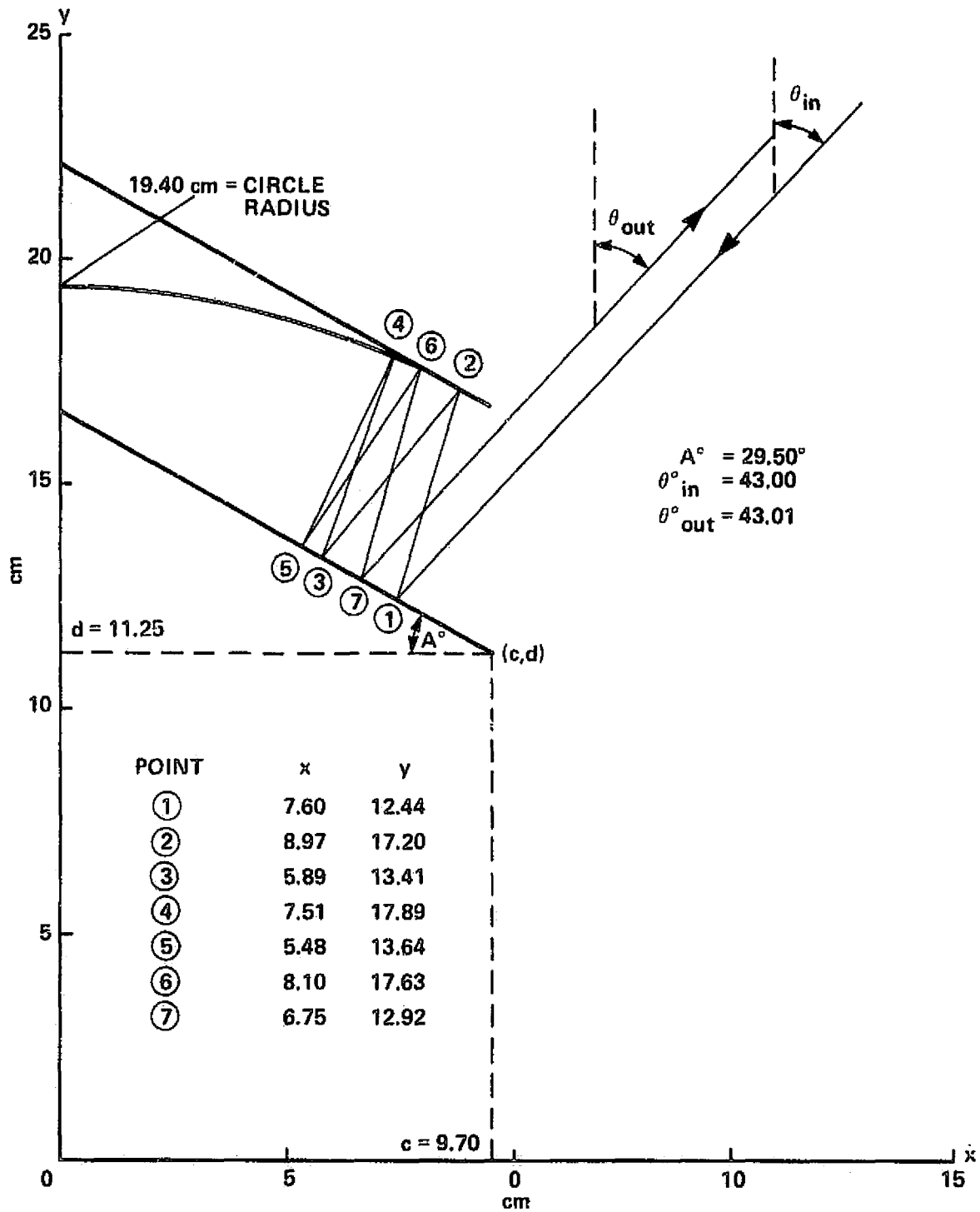


Figure 3.- Ray reflections for baffle angle of 29.50°.

ORIGINAL PAGE IS
OF POOR QUALITY

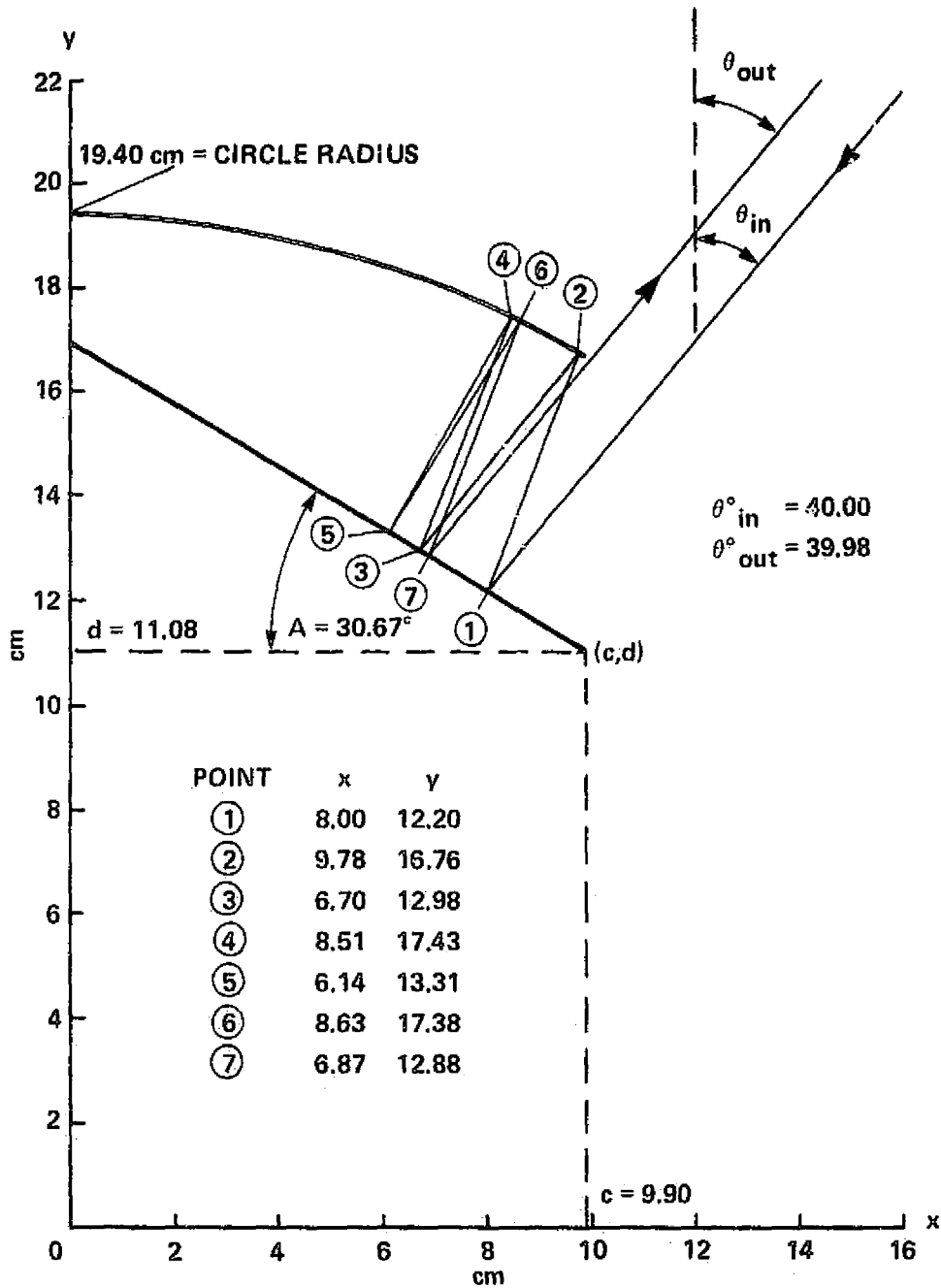


Figure 4.- Ray reflections for baffle angle of 30.67° .

ORIGINAL PAGE IS
OF POOR QUALITY

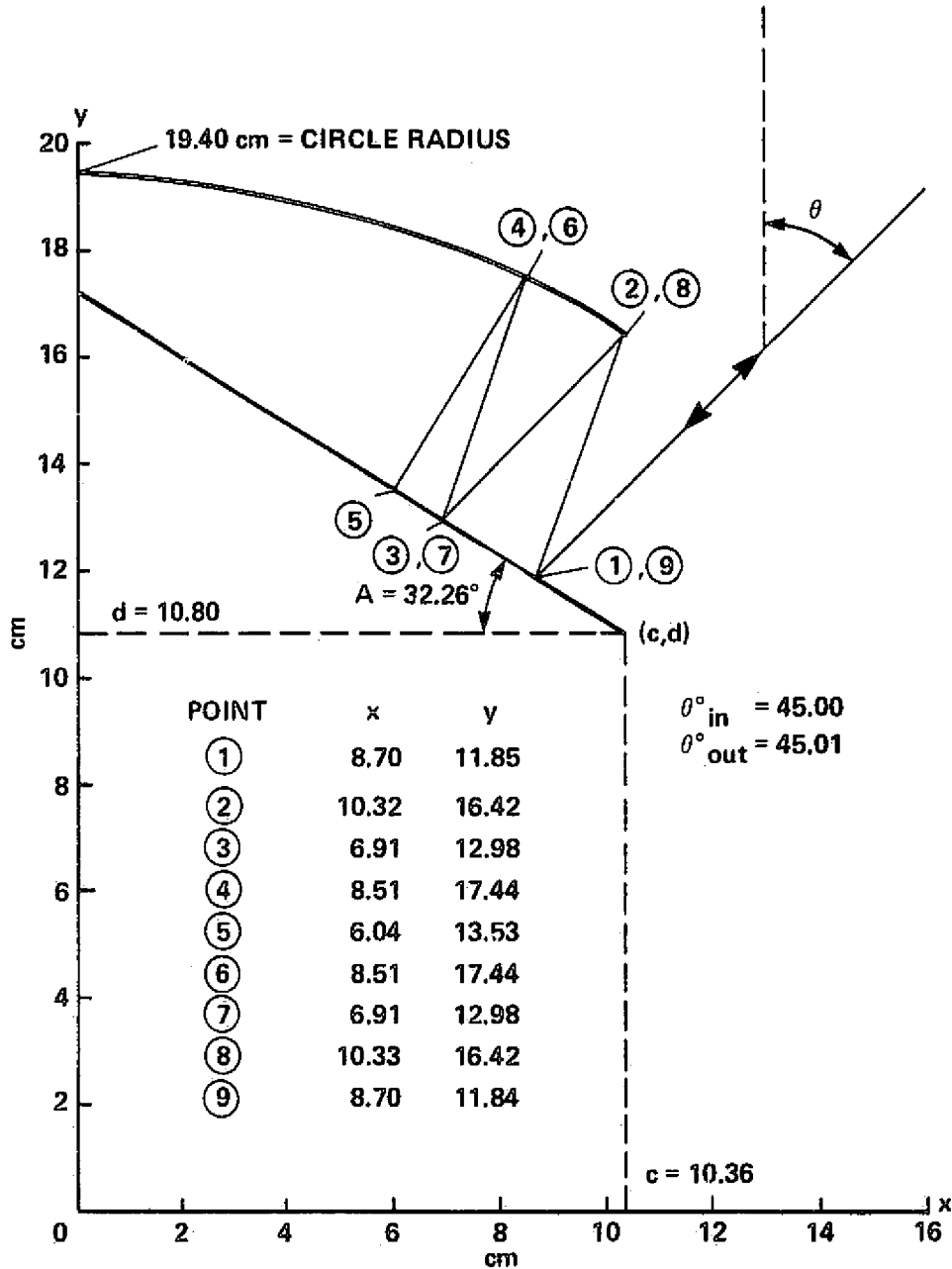


Figure 5.- Ray reflections for baffle angle of 32.26° .

ORIGINAL PAGE IS
OF POOR QUALITY

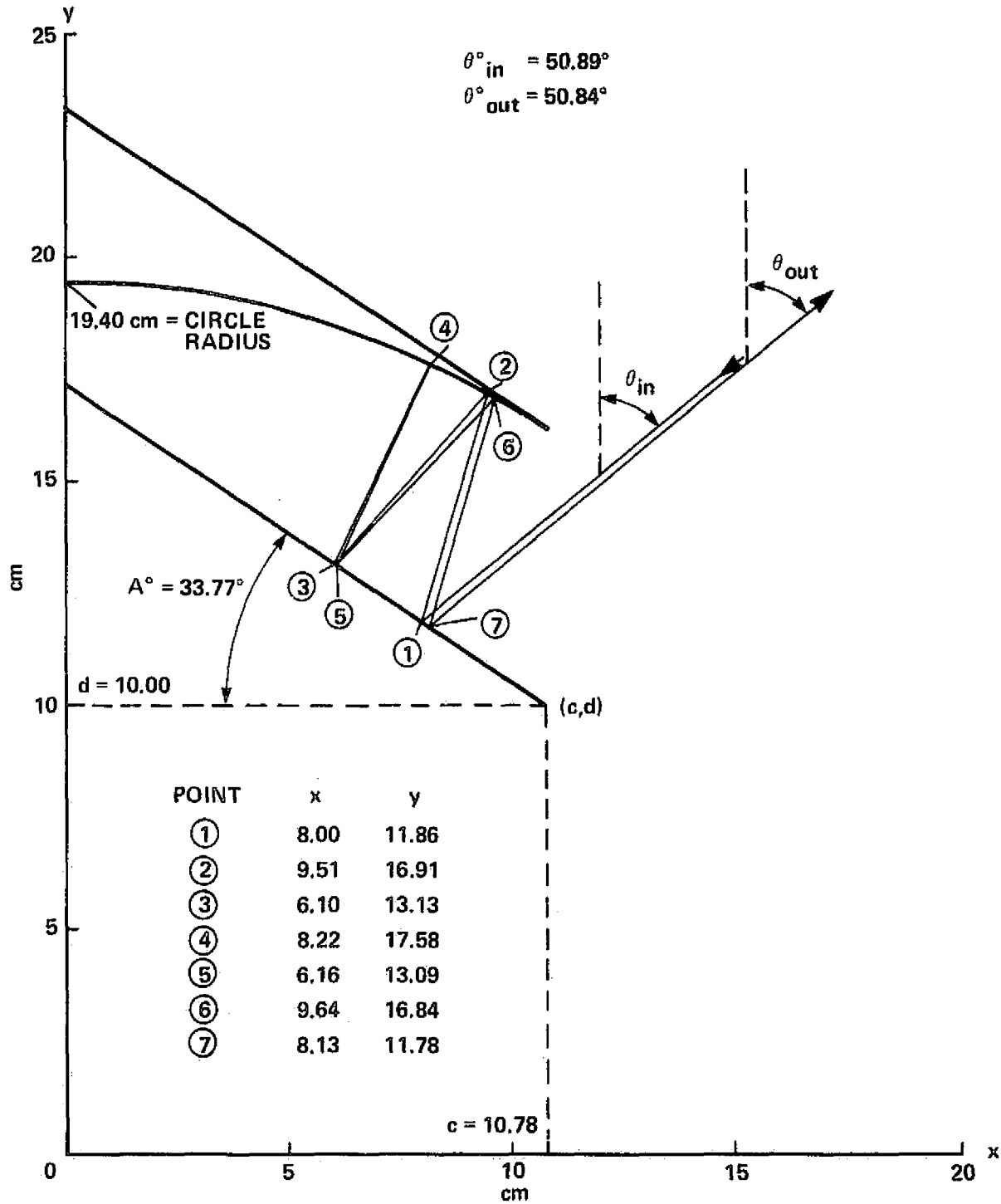


Figure 6.- Ray reflections for baffle angle of 33.77°.

ORIGINAL PAGE IS
OF POOR QUALITY

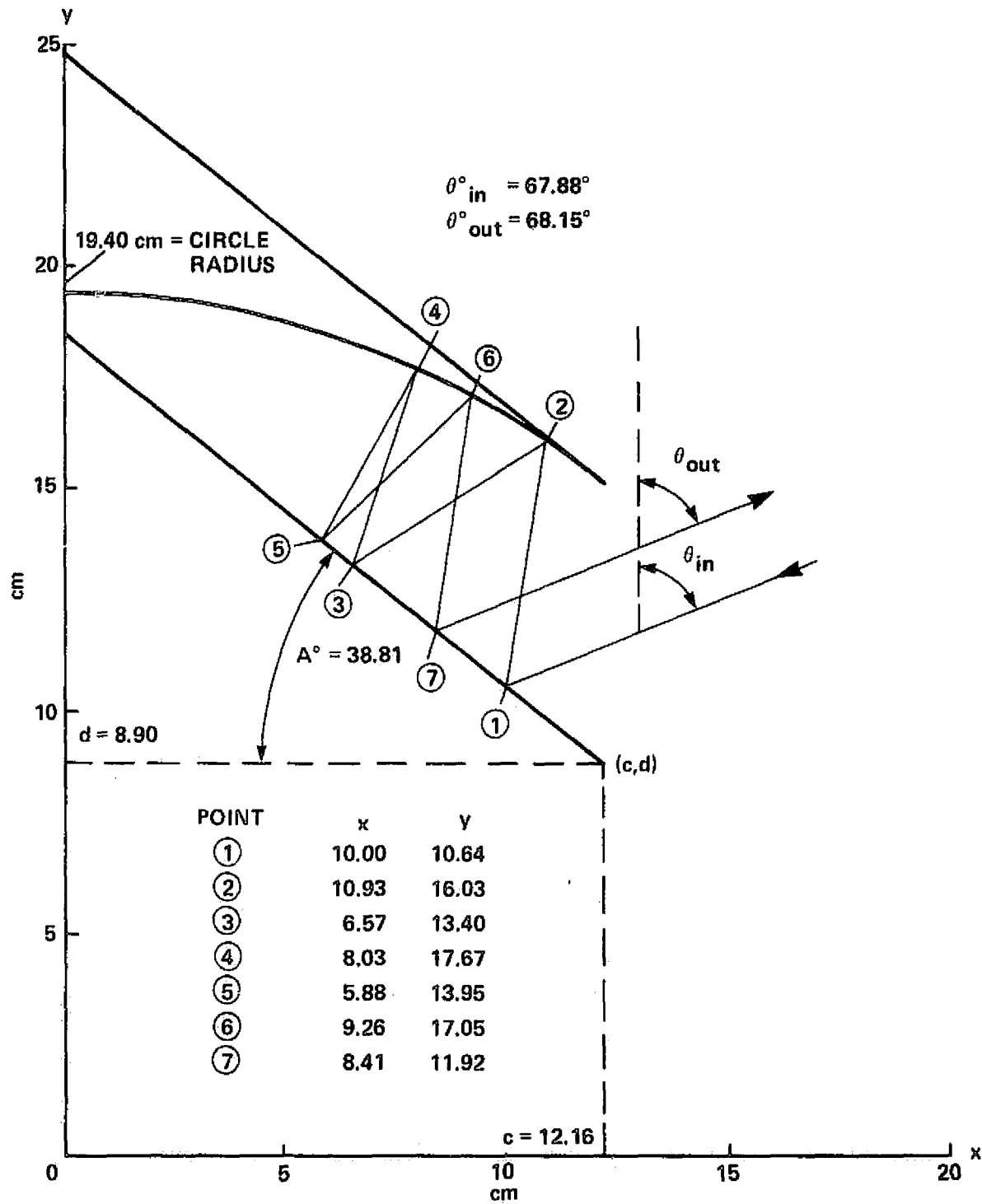


Figure 7.- Ray reflections for baffle angle of 38.81°.

ORIGINAL PAGE IS
OF POOR QUALITY

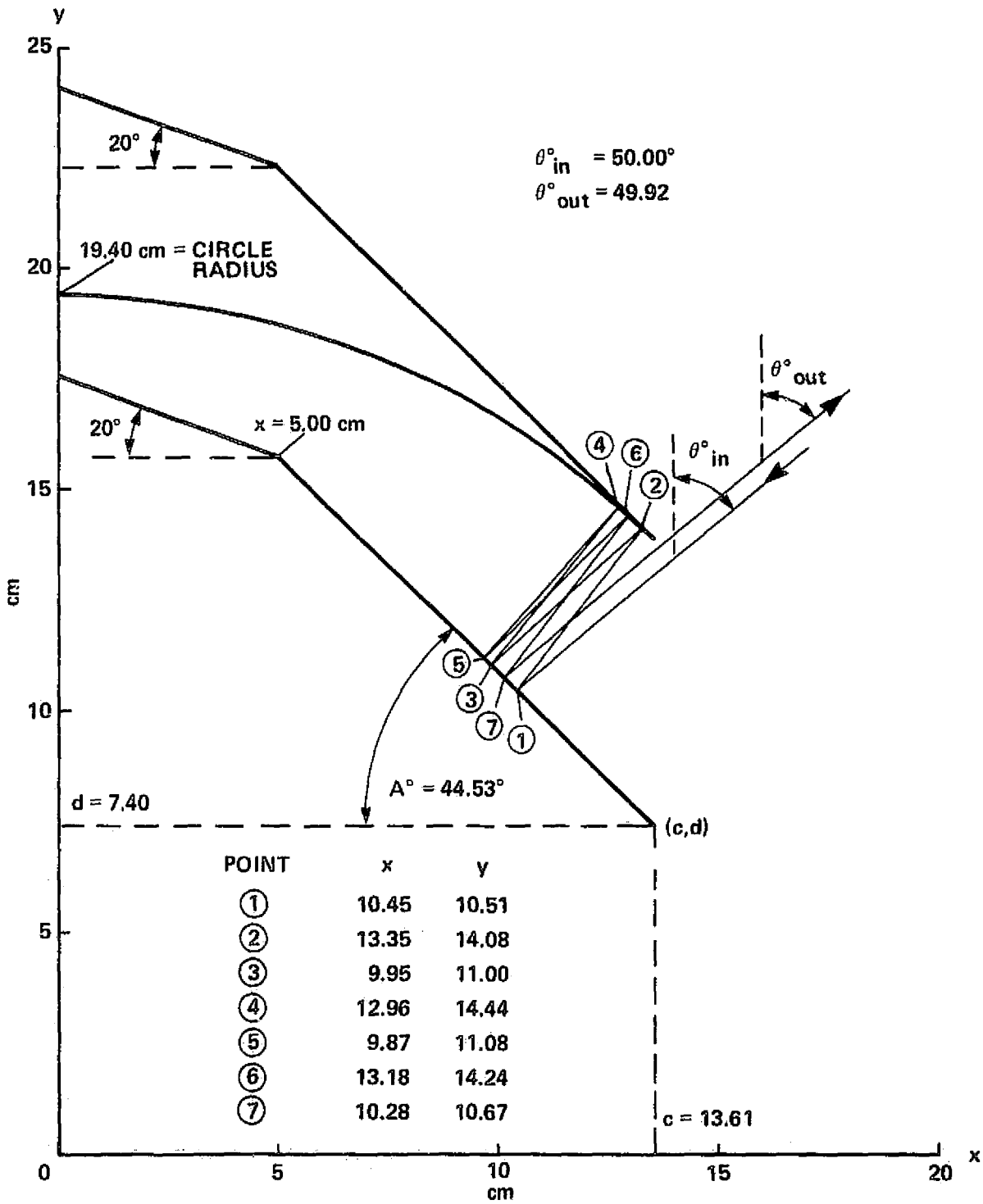


Figure 8. Ray reflections for baffle angle of 44.53° , and $\theta_{in} = 50.00^\circ$.

ORIGINAL PAGE IS
OF POOR QUALITY

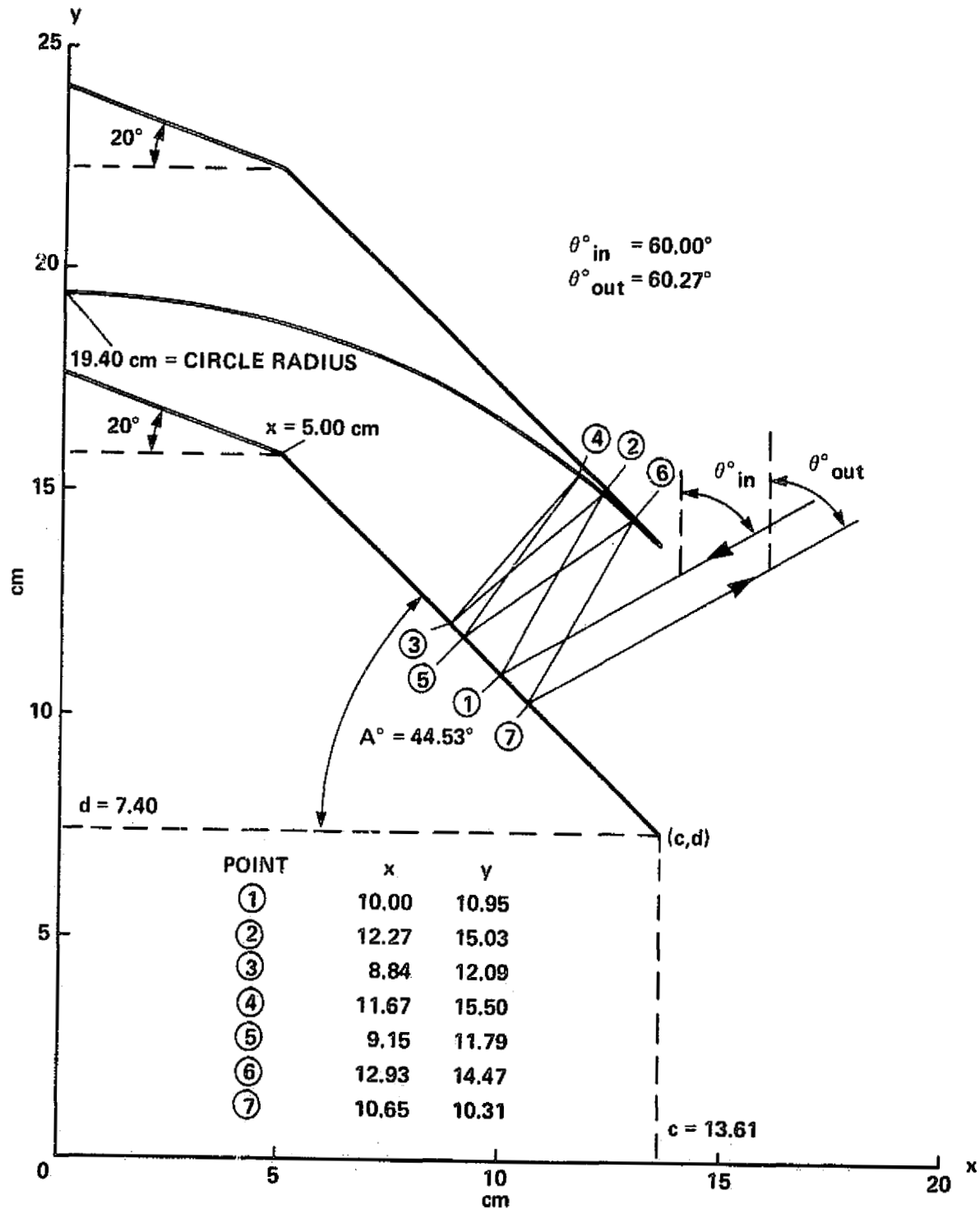


Figure 9.- Ray reflections for baffle angle of 44.53° , and $\theta_{in} = 60.00^\circ$.

ORIGINAL PAGE IS
OF POOR QUALITY

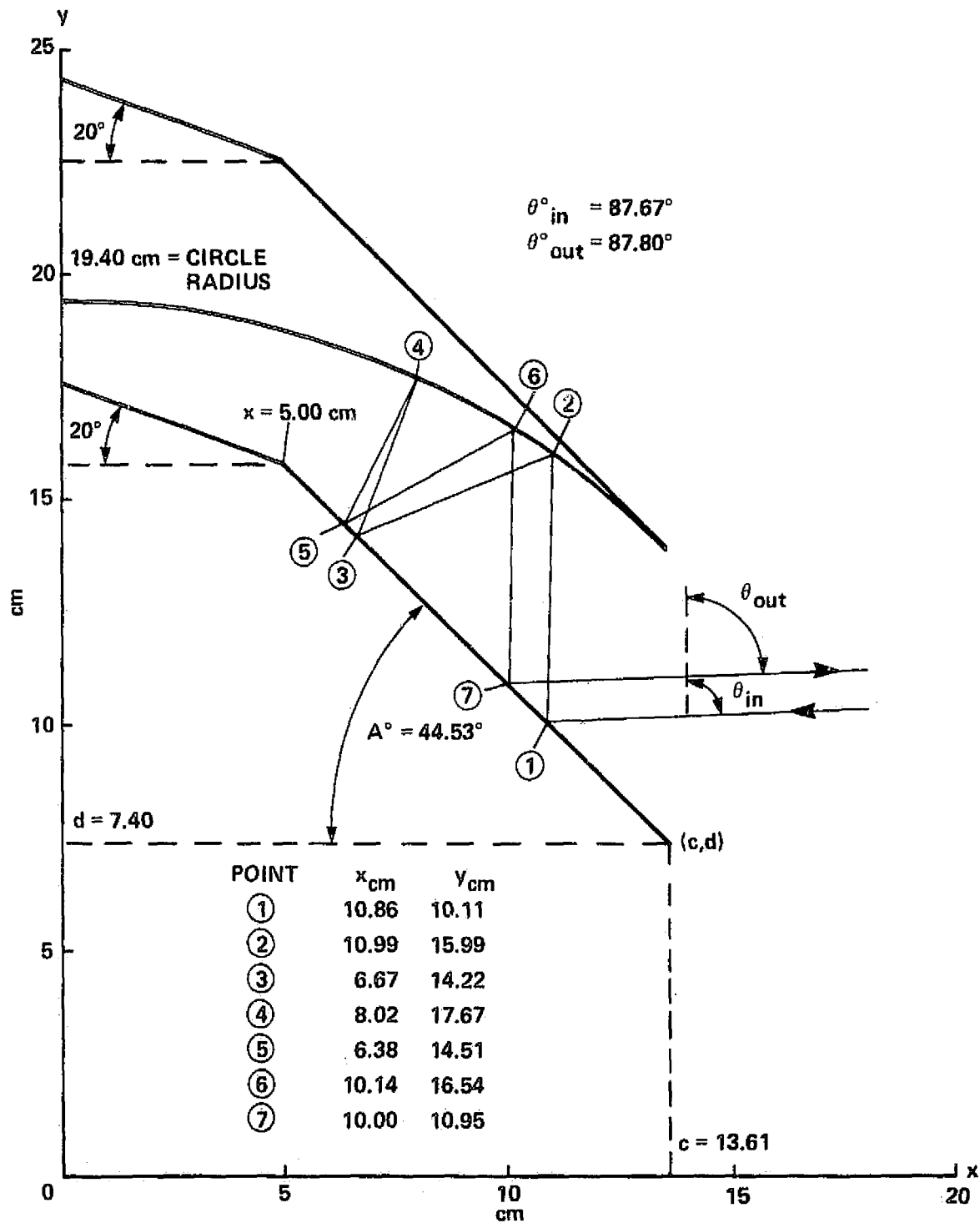


Figure 10.- Ray reflections for baffle angle of 44.53° , and $\theta_{in} = 87.67^\circ$.

ORIGINAL PAGE IS
OF POOR QUALITY

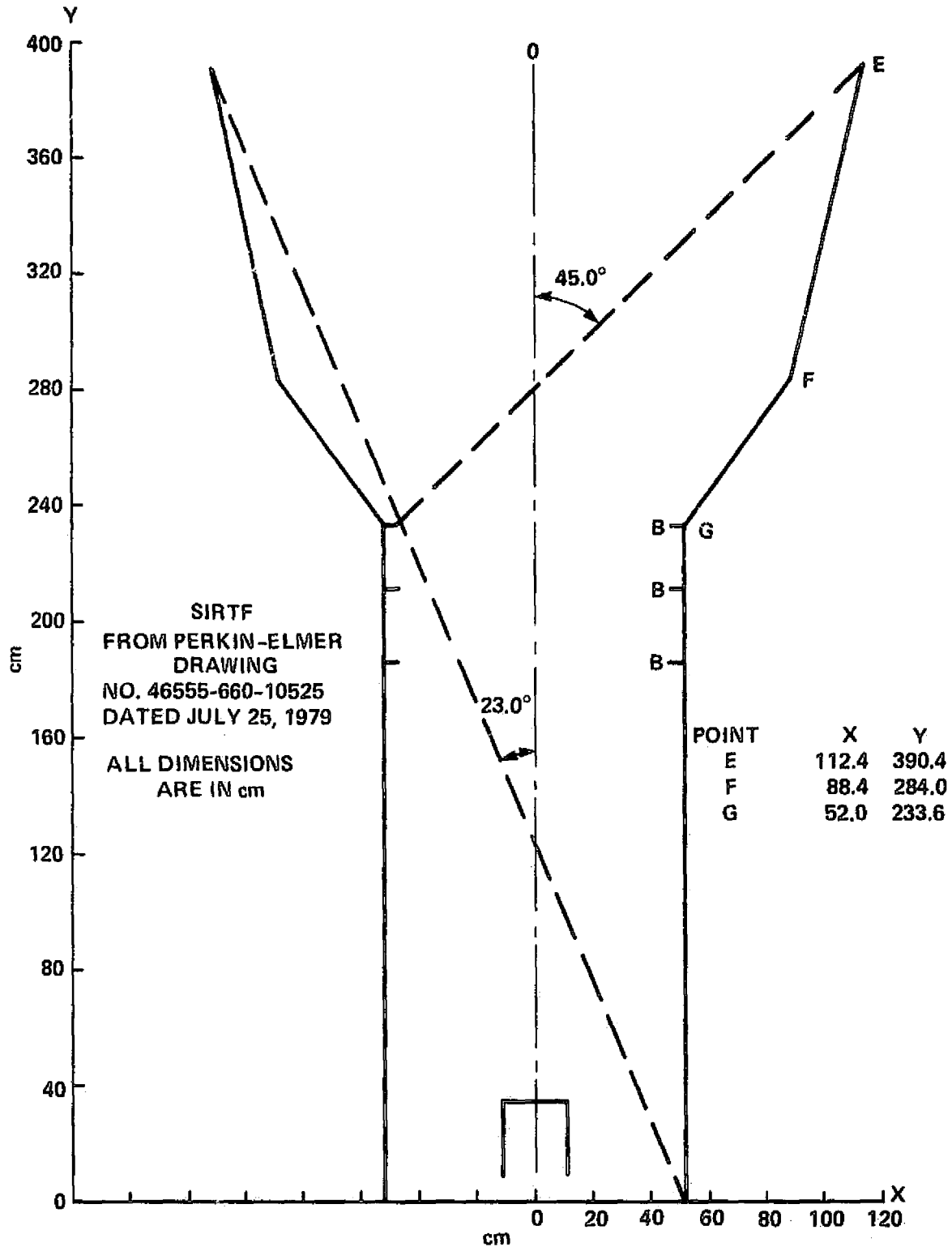


Figure 11.- Schematic outline of SIRTf telescope.

ORIGINAL PAGE IS
OF POOR QUALITY

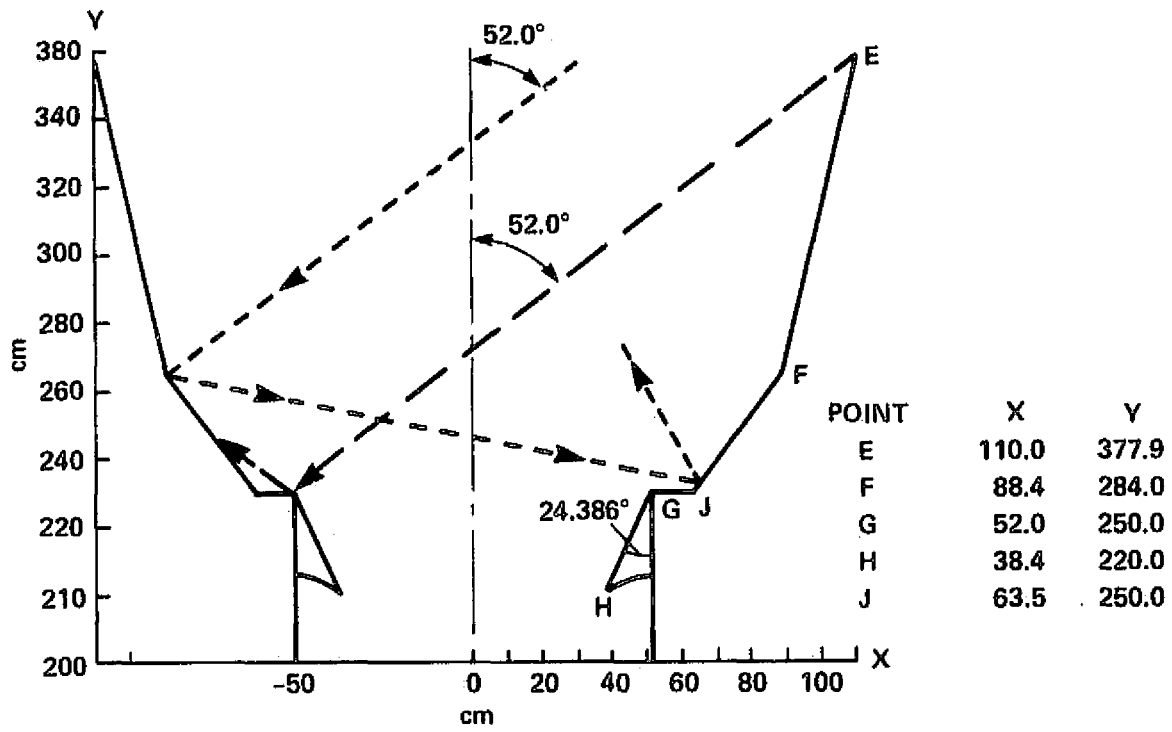


Figure 12.- Schematic outline of SIRIF sunshade, with $\theta_{in} = 52.00^\circ$.

ORIGINAL PAGE IS
OF POOR QUALITY

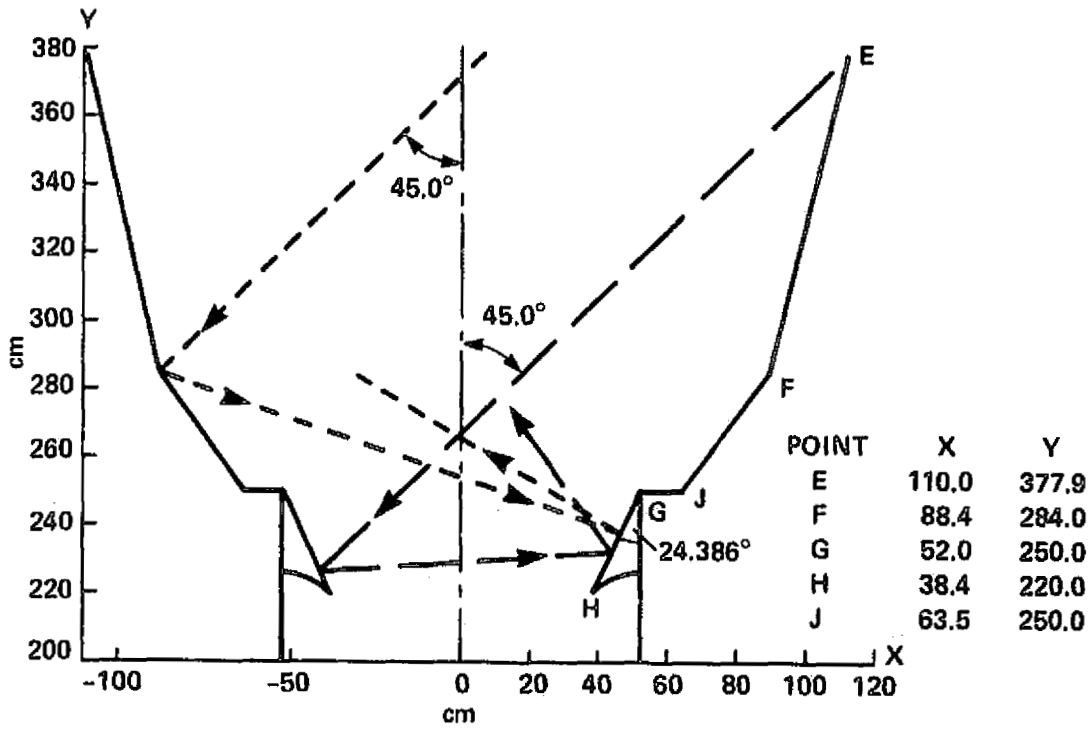


Figure 13.- Schematic outline of SIRTf sunshade, with $\theta_{in} = 45.00^\circ$.

ORIGINAL PAGE 18
OF POOR QUALITY

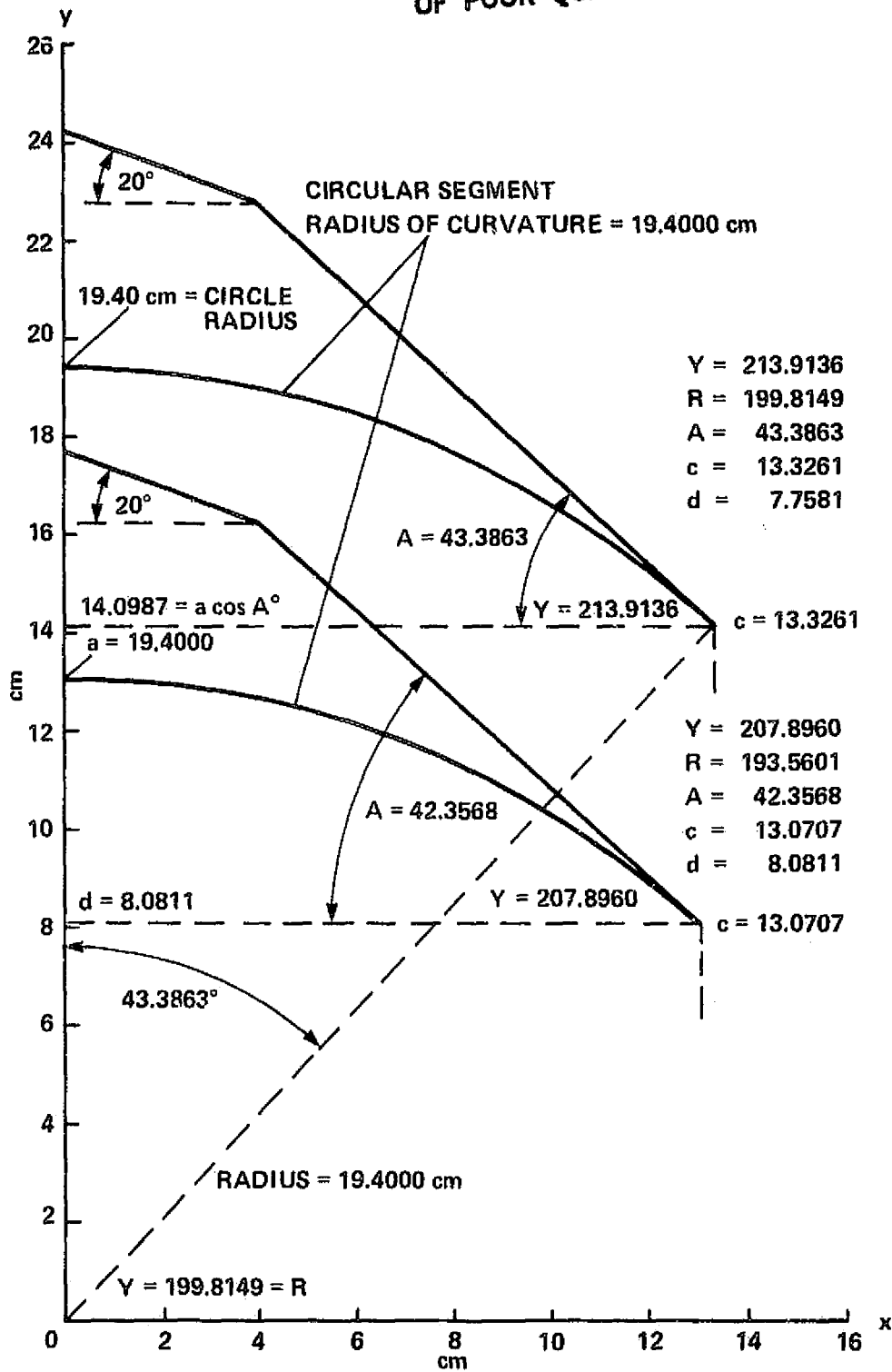


Figure 14.- Representative baffle design.

ORIGINAL PAGE IS
OF POOR QUALITY

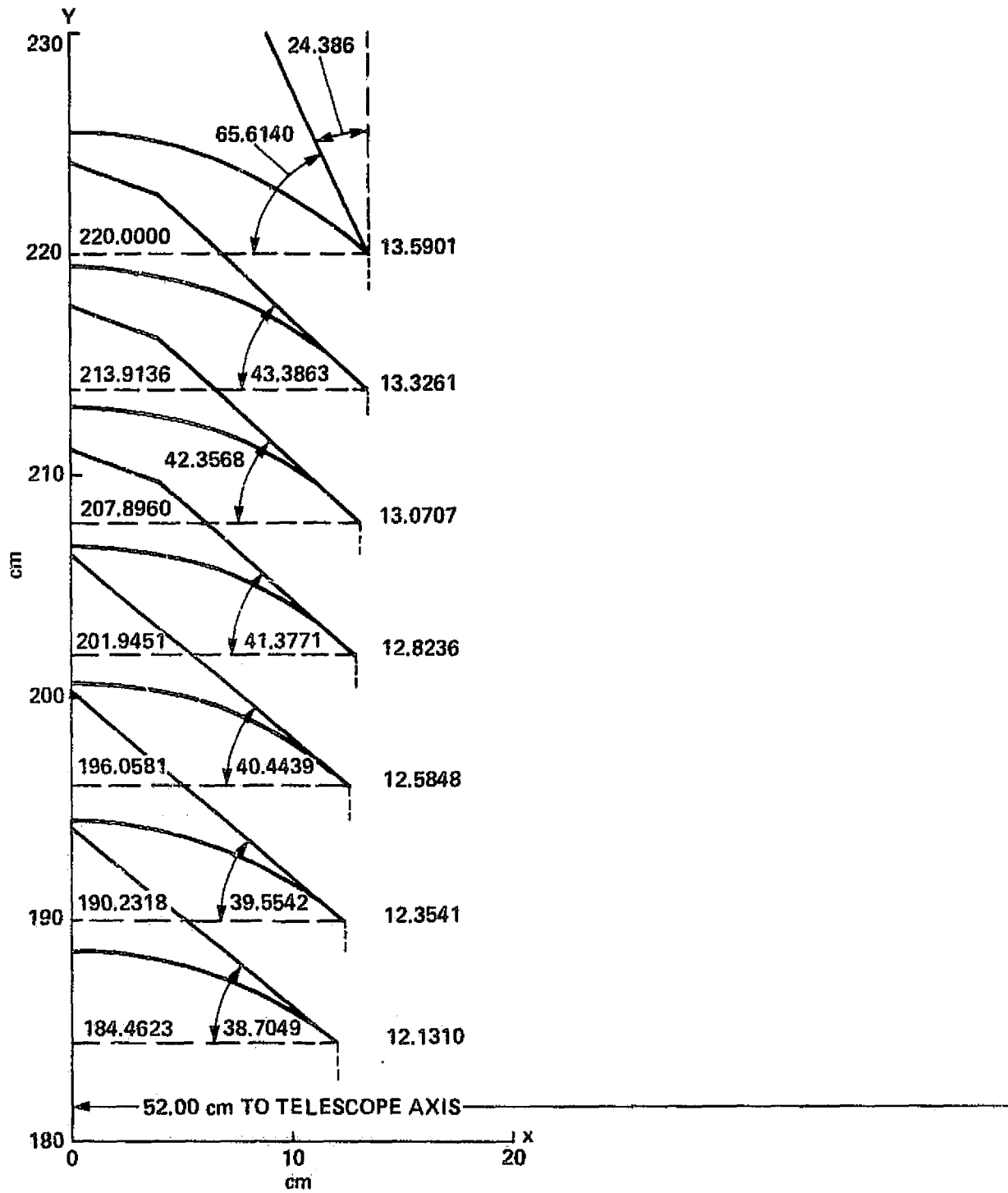


Figure 15.- Relationship of SIRTf baffles.

ORIGINAL PAGE IS
OF POOR QUALITY

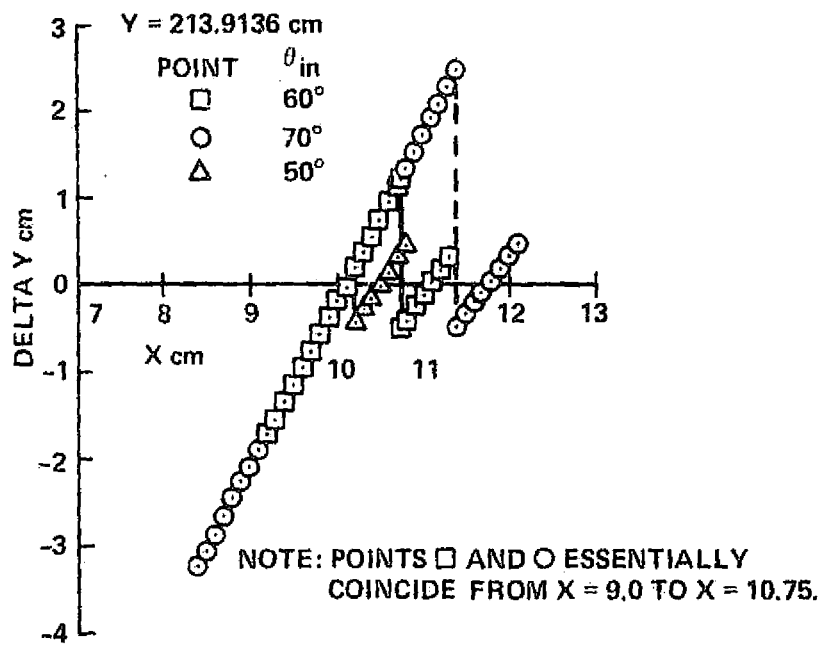


Figure 16.- Dependence of ray displacement on incoming ray angles.

ORIGINAL PAGE IS
OF POOR QUALITY

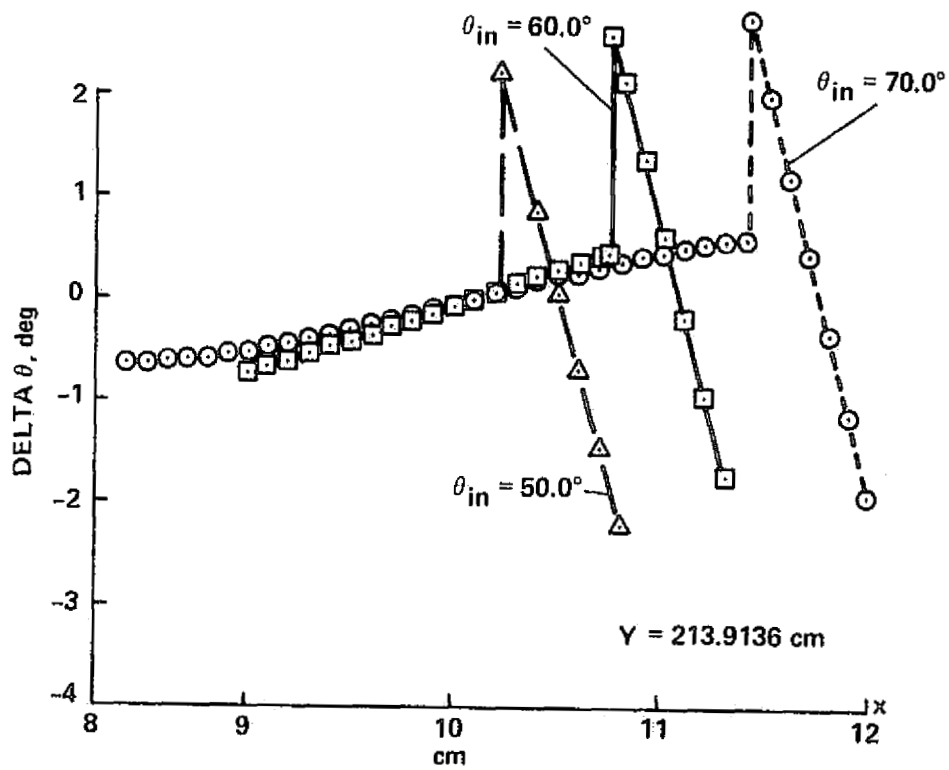


Figure 17.- Dependence of ray angular deviation on incoming ray angles.

ORIGINAL PAGE IS
OF POOR QUALITY

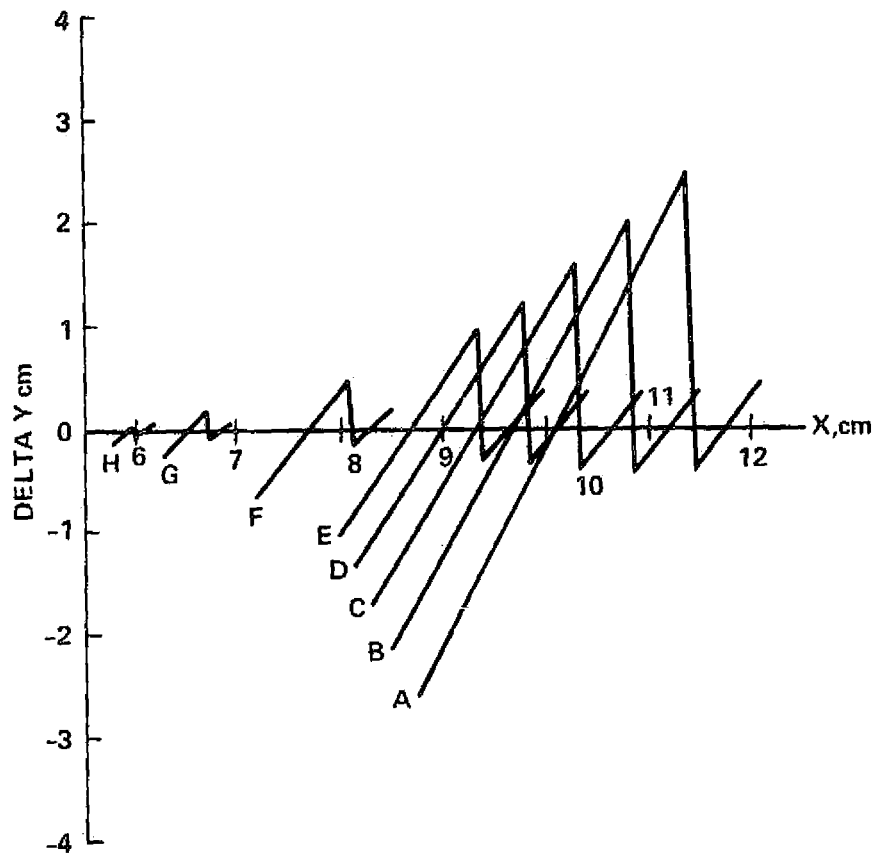


Figure 18.- Ray displacement for representative baffle sets.

ORIGINAL PAGE IS
OF POOR QUALITY

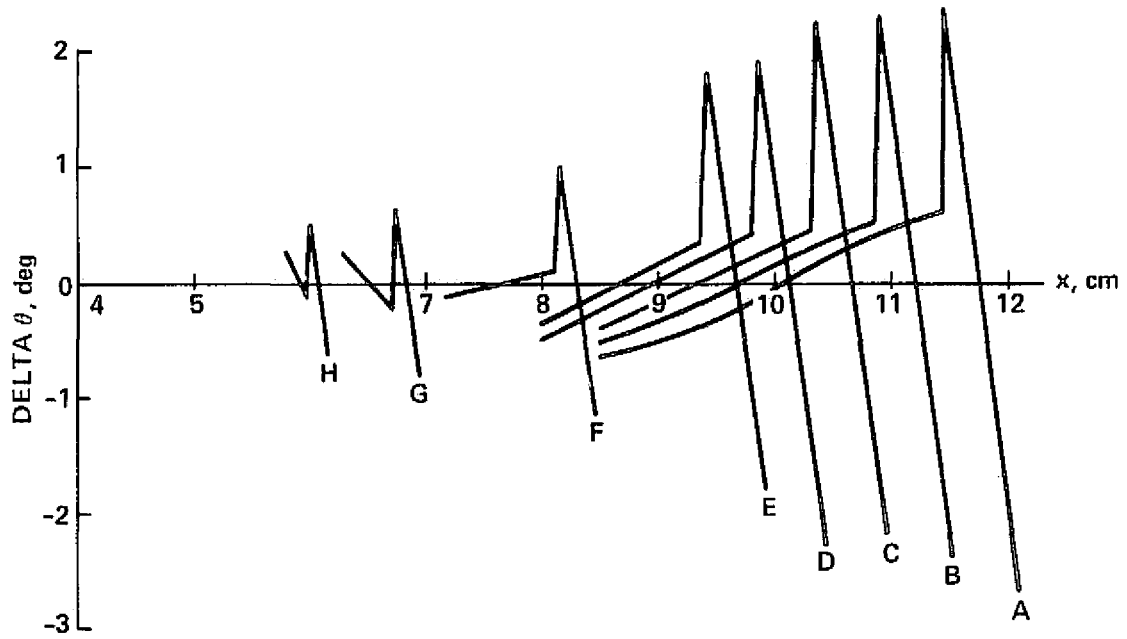


Figure 19.- Angular deviation of rays for representative baffle sets.

ORIGINAL PAGE IS
OF POOR QUALITY

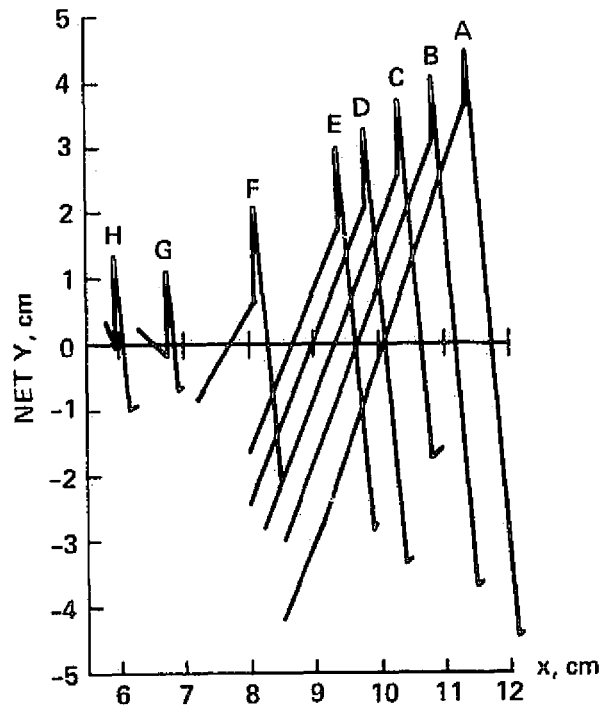


Figure 20.- Net displacement of rays for representative baffle sets.